Circ_0047339 promotes the activation of fibroblasts and affects the development of urethral stricture by targeting the miR-4691-5p/TSP-1 axis

Ke Ding
Xiangya Hospital Central South University
Daoyuan Li
Hainan General Hospital, Hainan Affiliated Hospital of Hainan Medical University
Rui Zhang
Hunan Traditional Chinese Medical College
Meilin Zuo (zuodabao@csu.edu.cn)
Second Xiangya Hospital of Central South University

Article

Keywords: urethral stricture, Circ_0047339, thrombospondin-1, miR-4691-5p, fibrosis

Posted Date: April 29th, 2022

DOI: https://doi.org/10.21203/rs.3.rs-1549681/v1

Abstract

Background

Urethral stricture is related to scar tissue fibrosis, but its pathogenesis is still unclear. This study aims to explore the mechanism of circular RNA (circRNA) in the occurrence and development of urethral stricture.

Methods

CircRNA microarray was employed to analyze circRNA expression profiles between human urethral scar tissue and normal urethral tissue. The first nine circRNA differentially expressed were selected for RT-qPCR detection. Urethral scar fibroblasts were isolated from human urethral scar tissue and cultured in vitro. The cells were transfected with si-circ_0047339, LV-circ_0047339, and miR-4691-5p mimic and their corresponding negative controls. Related gene and protein expression was measured by RT-qPCR, Western Blot and immunofluorescence staining, and the cell function was detected by CCK-8 and EDU assay. The targeting relationship between miR-4691-5p and circ_0047339 or TSP-1 was analyzed by dual-luciferase reporter assay.

Results

The results of circRNA microarray showed that there were 268 differential genes between urethral scar tissue and normal urethral tissue (circRNA expression difference multiple ≥ 2 and p value ≤ 0.05). The enrichment analysis of KEGG (Kyoto encyclopedia of genes and genomes) showed that these circRNAs were significantly correlated with ECM-receptor interaction. The first nine differentially expressed circRNA were selected to predict the circRNA-miRNA network. RT-qPCR results showed that circ_0047339 was upregulated considerably in urethral scar tissue. After silencing circ_0047339, the proliferation of urethral scar cells decreased significantly, and the expression of collagen 1 (COL-1) and α-smooth muscle actin (α-SMA) also reduced. Circ_0047339 as a competing endogenous RNA (ceRNA) could increase the expression of TSP-1 by competitively binding miR-4691-5p. In addition, miR-4691-5p mimic transfection could inhibit the proliferation of urethral scar fibroblasts and the presentation of thrombospondin-1 (TSP-1), α-SMA and COL-1, while circ_0047339 overexpression eliminated this inhibition.

Conclusion

Our results showed that the dysfunctional circ_0047339 might promote the growth and fibrosis of urethral scar fibroblasts through the ceRNA mechanism, thus promoting the development of urethral stricture via miR-4691-5p/TSP-1 axis.

1 Introduction

Urethral stricture is a narrowing of the urethra related to fibrosis scar formation, which is a relatively common disease in urology practice. Its incidence rate in susceptible populations is estimated to be 0.6% [1, 2]. It will lead to obstructive and irritating urinary symptoms, damage the whole urinary tract, and eventually lead to the loss of renal function, which seriously reduces patients' quality of life [3]. With the development of modern medicine and surgery, various surgical options can be used to treat urethral stricture, including urethral dilatation, urethrotomy, and urethroplasty [4, 5]. However, the current surgical treatment shows a high failure rate due to the new epithelial damage and the elimination of concentric fibrous scars in the lumen [6]. Among them, the failure rate of urethral dilatation and urethrotomy is as high as 90%, and the long-term effect is poor [7, 8], and 25% of urethroplasty recurs after 6 months [9]. Therefore, it is an urgent problem to study a new treatment for urethral stricture.

The pathophysiology of urethral stricture is mostly unknown. Fibrosis of urethral mucosa and surrounding corpus cavernosum after infectious, inflammatory or traumatic injury may lead to stenosis [10, 11]. Pathogenesis includes fibroblast proliferation, collagen synthesis and extracellular matrix (ECM) deposition [12]. Thrombospondin-1 (TSP-1) is an ECM glycoprotein, which can mediate cell-matrix and cell-cell interactions [13]. TSP-1 is an endogenous activator of transforming growth factor-beta (TGF-beta), which is involved in developing many fibrosis diseases, including liver fibrosis, renal fibrosis and fibrosis complications of multiple myeloma [14, 15]. Eliminating TSP-1 function in renal fibrosis induced by unilateral ureteral obstruction (UUO) can prevent interstitial fibrosis [16]. However, it is not clear whether TSP-1 is involved in the occurrence and development of fibrosis in urethral stricture.

Gene therapy has become a promising treatment option for many diseases [17]. Circular RNA (circRNA) is a new endogenous non-coding RNA that has attracted research interest [18]. Many evidence shows that circRNA is involved in many disease processes, including renal and liver fibrosis [19, 20]. In the reports of fibrosis-related diseases, such as myocardial fibrosis [21], diabetic nephropathy [22] and pulmonary fibrosis [23], it has been revealed that circRNA acts as a molecular sponge, which can isolate miRNA molecules and prevent the mechanism of targeting mRNA. However, there is little research on the role of circRNA in urethral fibrosis.

Therefore, this study aims to increase the information about circRNA imbalance in urethral fibrosis to broaden the understanding of the underlying pathological mechanism and find new therapeutic targets. Through circRNA sequencing, temporary circRNA expression profiles were generated in the urethral scar and normal urethral tissue, then differentially expressed circRNA was obtained. CircRNA-miRNA targeting TSP-1 was selected for interaction. Through basic experiments, the mechanism of circRNA-miRNA targeting TSP-1 in urethral fibrosis was clarified to provide a new target and theoretical basis for treating urethral fibrosis-related diseases.

2 Materials And Methods

2.1 Source of clinical specimens

From the month of Jan. 2021 to Jun. 2021, six pairs of the urethral scar and normal urethral tissue were collected in Xiangya Hospital Central South University. Informed consent was obtained from all subjects and their legal guardians.Patients' baseline information was summarized in Table 1. Before the operation, the materials were local without infection and ulcer and were not treated with drugs or radiotherapy. All specimens were obtained with the consent of patients and their families before operation and confirmed by pathological examination. The procedure used in this research followed the tenets of the Declaration of Helsinki and was approved by Medical Ethics Committee of Xiangya Hospital Central South University.

Table 1
Patient demographics in this study.

Number of subject	Age	Gender	Etiology
1	61	male	trauma
2	56	male	trauma
3	71	male	iatrogenic
4	43	male	trauma
5	48	male	trauma
6	52	male	trauma

2.2 CircRNA microarray analysis

The circRNA expression profile of the urethral scar and normal urethral tissue was detected using CapitalBio Technology Human CircRNA Array v2 (CapitalBio Technology, China). The total RNA of three urethral scar tissue and three normal urethral tissue were extracted. The purity and concentration of the RNA were determined by a NanoDrop ND-1000 instrument (Thermo Scientific, USA). The extracted RNAs were amplified and reverse transcription into cDNA, then labeled with Cy3-dCTP. After purification, the labeled DNAs were hybridized to a microarray (CapitalBio Technology Human CircRNA Array v2). The circRNAs expression difference and statistical significance P value were calculated by GeneSpring GX software. Cluster analysis and graphical display with Cluster3.0 software. According to the grouping information, the differential comparison is conducted to obtain differential genes. Kyoto encyclopedia of genes and genomes (KEGG) Pathway analysis was performed on the linear mRNA transcripts corresponding to different circRNA, and the miRNA that circRNA might bind to was predicted.

2.3 Primary cell extraction and culture

The urethral scar tissue or normal urethral tissue was repeatedly rinsed in PBS containing antibiotics to remove redundant epithelial tissue. The tissues were divided into small pieces of 5 mm×5 mm in size and dropped the culture medium was onto the tissue to keep it moist. The tissues were put into a centrifuge tube, added 0.25% trypsin digestive juice -EDTA and collagenase, digested in a constant temperature water bath at 37℃ for 4 ~ 5 hours, and shaken once every hour. Filter the suspension with a filter screen, take the filtered suspension for centrifugation, discard the supernatant, add 6 mL of fresh culture

solution, and culture in a cell incubator at 37℃ and 5% CO_2. The next day, most of the fibroblasts adhered to the wall, the cell culture medium was changed, and the cells were changed every 2 ~ 3 days. Finally, urethral scar fibroblasts and normal urethral fibroblasts were successfully separated and cultured. The α-smooth muscle actin (α-SMA) was selected as a marker of fibroblasts for detection.

2.4 Cell transfection

The small interference RNA (siRNA) specifically targeting circ_0047339 (si-circ_0047339), Lentivirus harboring circ_0047339 (LV-circ_0047339), miR-4691-5p mimic and their corresponding negative controls (si-NC, vector, mimic NC) were obtained from honorgene Company (Changsha, China). According to the manufacturer's protocol, cells were transfected with Lipofectamine 3000 reagent (ThermoFisher, USA) [24].

2.5 Western blot

Total protein was extracted from the collected cells by RIPA lysate (AWB0136, Abiowell) containing protease inhibitor (583794, Jintai Hongda, Beijing, China) and protein phosphatase inhibitor (AWH0650, Abiowell). Then, the protein was transferred to the NC membrane after 10% SDS-PAGE treatment. The membrane was sealed with 5% skim milk (AWB0004, Abiowell) at room temperature for 2 hours. collagen I (COL-1, 1: 10000, 67288-1-Ig, proteintech), α-SMA (1: 6000, 14395-1-AP, proteintech), TSP-1 (1: 1000, 18304-1-AP, proteintech), β-actin (1: 5000, 66009-1-Ig, proteintech) were added. Then, the corresponding secondary antibodies HRP goat anti-mouse IgG (1: 5000, SA00001-1, proteintech) or HRP goat anti-rabbit IgG (1: 6000, SA00001-2, proteintech) were incubated with the membrane at room temperature for 2 hours. The membrane was incubated with SuperECL Plus (AWB0005, abiowell), and then the protein bands were visualized by Chemiluminescence imaging system (Chemiscope 6100, Clinx, China). The relative content of protein is expressed as target protein / β-actin.

2.6 Quantitative reverse transcription PCR (RT-qPCR)

Trizol kit (15596026, Thermo) was adopted to extract the total RNA of cells, and RNA was reverse transcribed into cDNA by reverse transcription kit (CW2569, CW2141, Beijing Kangwei Century). RT-qPCR was carried out under the following reaction conditions using UltraSYBR Mixture (CW2601, Beijing Kangwei Century), cDNA and primers. 95°C 10min, 95°C 15 s, 60℃ 30 s, 40 cycles. GAPDH is the internal control of genes, and U6 is the internal control of miRNAs. The formula is $2^{-\Delta\Delta Ct}$. The primers used in this study are Table 2.

Table 2
Primer sequences

Gene	Sequences (5'-3')
hsa_circ_0005413	forward: GGACCTCTTTCAATGACAACGC
	reverse: CCATCTGTTGCCAAACCACT
hsa_circ_0006912	forward: AGCCTACTGCAAATCCAAACAC
	reverse: CAGGTTTCTTGCCTCTTGGTT
hsa_circ_0019957	forward: AAAACATGCCCCAGAGTCCT
	reverse: ACACTTGCCGATCGACTCCC
hsa_circ_0021726	forward: GGACCTCTTTCAATGACAACGC
	reverse: CATCATCAATGCCTGATCCAGA
hsa_circ_0021731	forward: TTCAACCCAATCTCACACCCC
	reverse: GGTGCCATTTCTGTCTACATGC
hsa_circ_0047338	forward: TTATCCCAGTTCCTGATGGCT
	reverse: TCCCACTCCAGAGATTCGGTA
hsa_circ_0047339	forward: CCATGAGAACAAGGCATTCCAC
	reverse: CTCCCGGTCGACTATAGCTG
hsa_circ_0047343	forward: TAACAGCCAATGGAGCCGAT
	reverse: TGTTCTAGCGGAGACAACCAC
hsa_circ_0093740	forward: CACTTATCAAGCTGCCATACCTG
	reverse: GGTCCTCCAGCAGTCCCTT
TSP-1	forward: AAACACTGAAGCACACGCAAC
	reverse: GACAGCTCCTCCCTCATCCAC
hsa-let-7b-5p	forward: ACAGCAGGCACAGACAGGCAGT
	reverse: GCTGTCAACGATACGCTACGTAA
hsa-miR-4691-5p	forward: ACAGCAGGCACAGACAGGCAGT
	reverse: GCTGTCAACGATACGCTACGTAA
hsa-miR-550b-2-5p	forward: ACAGCAGGCACAGACAGGCAGT
	reverse: GCTGTCAACGATACGCTACGTAA
hsa-miR-766-5p	forward: ACAGCAGGCACAGACAGGCAGT

Gene	Sequences (5'-3')
	reverse: GCTGTCAACGATACGCTACGTAA
GAPDH	forward: ACAGCCTCAAGATCATCAGC
	reverse: GGTCATGAGTCCTTCCACGAT
U6	forward: CTCGCTTCGGCAGCACA
	reverse: AACGCTTCACGAATTTGCGT

2.7 Immunofluorescence (IF) analysis

COL-1 and α-SMA expressions were measured by IF analysis. Simply put, the cell slides were fixed with 4% paraformaldehyde for 30 minutes, washed with PBS 3 times and blocked with 5% BSA at 37°C for 60 minutes. The slides were incubated with the first antibody (COL-1 (1: 50, 67288-1-IG, proteintech), α-SMA (1: 50, AB7817, abcam)) at 4℃ overnight. Then, the CoraLite594-conjugated Goat Anti-Mouse IgG (H + L) (1:200SA00013-3, proteintech) antibody was incubated with the slides at 37℃ for 90 min. DAPI working solution was stained at 37℃ for 10 min. The results were observed under a microscope (BA210T, Motic).

2.8 Cell Counting Kit-8 (CCK-8) assay

According to the manufacturer's instructions, the CCK-8 kit (NU679, DOJINDO) was used to detect cell viability. The cells were inoculated into a 96-well plate (1× 10^4/well) and attached to the wall in a 5% CO2 incubator at 37℃ for 24 hours. According to the demand, the cells were divided into groups. Each group was provided with 6 compound holes 24 hours after taking out the 96-well plate, observing it under a microscope, adding CCK-8 reagent and incubating for 2 hours. A microplate analyzer was utilized to detect the absorbance (OD) value at 450 nm, and the results were recorded.

2.9 5-Ethynyl-2'-deoxyuridine (EDU) assay

According to the manufacturer's instructions, cell proliferation was caught by the EDU assay kit (Guangzhou RiboBio). The cells were inoculated into 96-well plates (1×10^4/ well) and incubated with 4% paraformaldehyde at room temperature for 30 minutes. Then, the cells were treated with 100 μL of 1 × Apollo® staining reaction solution for 30 min. Next, 100 μL Hoechst 33342 reaction solution was added to each well and incubated for 30 minutes. Immediately after dyeing, we used a microscope (DSZ2000X, Beijing Cnmicro instrumentco., Ltd) to observe and take pictures.

2.10 Dual-luciferase reporter assay

According to the manufacturer's instructions, circ_0047339 wide type (WT) or circ_0047339 mutant (MUT) or TSP-1-3' UTR WT or TSP-1-3' UTR MUT, and miR-4691-5p mimic or NC mimic were co-transfected in 293A cells (HonorGene, Changsha) with Lipofectamine 300 transfection reagent (Invitrogen). The cells were digested with trypsin, centrifuged and discarded the supernatant. The luciferase activity was measured using a Dual-luciferase assay kit (E1910, Promega, USA).

2.11 Statistics

Statistical analyses were conducted using GraphPad Prism 9 software (GraphPad Software, Inc., USA). Each experiment was conducted at least three times. Statistical analysis among more than two groups and between two groups was performed using ANOVA and Student's t-test. Data are presented as means ± standard deviations. P-value < 0.05 was considered significant.

3 Results

3.1 CircRNA expression profile analysis of urethral scar tissue

We performed circRNA microarray to identify the differential circRNA expression between human urethral scar tissue and normal urethral mucosa tissue and determined the characteristics of circRNA in the urethral scar. Principal Component Analysis (PCA) was a statistical method to reflect the similarity of samples. By dimensionality reduction of data, the expression of samples was displayed in three-dimensional space. The result showed that the contribution rate of the top 3 principal components is 77.52% (Fig. 1A). The scatter plot showed the signal values of the experimental and control samples, and it could be intuitively seen that there was a significant difference in gene expression between the urethral scar group and the normal urethral mucosa tissue samples (Fig. 1B). In addition, we drew a volcano map together with P-value and FC value obtained by difference analysis. When the expression difference multiple of circRNA in two groups of samples was ≥ 2 and P-value was ≤ 0.05, it was defined as a differential gene, and 296 differential circRNA were identified (Fig. 1C). Among them, 166 circRNA expressions were down-regulated, and 130 circRNA expressions were upregulated in human urethral scar tissue compared with normal urethral tissue.

3.2 Interaction between circRNA and miRNA in urethral scar tissue

In order to further explore the functional changes caused by circRNA changes in patients with urethral fibrosis, based on the microarray analysis data, KEGG pathway of different circRNA groups was annotated and enriched. KEGG pathway statistical chart showed the first 30 enriched signal pathways (Fig. 2A). Statistical analysis shows that the differential circRNA was significantly related to ECM-receptor interaction, Arrhythmogenic right ventricular cardiomyopathy (ARVC), Thyroid hormone synthesis, Proteoglycans in cancer and Focal adhesion. CircRNA could combine with miRNA in a targeted way and indirectly regulate the translation of mRNA [25]. Using miRanda software, the differentially expressed circRNA was selected to predict the target miRNA, and the circRNA-miRNA network diagram was drawn. The results showed the interaction between the first ten most significantly expressed circRNA and its target miRNA (Fig. 2B).

3.3 The expression of circ_0047339/miRNA/TSP-1 interaction in urethral scar tissue

We collected human normal urethral tissue and human urethral scar tissue, and determined the expressions of COL-1 and α-SMA via western blot assay. The results showed that the expressions of COL-1 and α-SMA were significantly upregulated in human urethral scar tissue compared with normal urethral tissue (Fig. 3A). Next, we verified the expression of the first nine differential circRNA in the microarray analysis results by RT-qPCR. The results showed that circ_0047339 was upregulated in human urethral scar tissue, and the most significant difference (Fig. 3B). Therefore, we choose circ_0047339 for follow-up research. Then, the expression of target miRNA of circ_0047339 in human urethral scar tissue was detected by RT-qPCR. The results showed that miR-766-5p and miR-4691-5p in human urethral scar tissue were down-regulated (Fig. 3C). While miR-550b-2-5p and let-7b-5p were the opposite. Among them, miR-4691-5p has the most significant difference. In addition, we also detected the expression of TSP-1. The results showed that TSP-1 urethral scar tissue expression was upregulated compared with normal urethral tissue (Fig. 3D). The above results indicated that there might be a sponge mechanism of circ_0047339 / miR-4691-5p / TSP-1 in human urethral scar tissue.

3.4 Circ_0047339 regulated the fibrosis of urethral fibroblasts

Next, to study the function of circ_0047339, we extracted human primary urethral fibroblasts and human primary urethral scar fibroblasts. IF detection showed that the expression of COL-1 and α-SMA in human primary urethral scar fibroblasts increased more than those in human primary urethral fibroblasts (Fig. 4A). The results of RT-qPCR showed that circ_0047339 and TSP-1 were upregulated in human primary urethral scar fibroblasts, while miR-4691-5p was the opposite (Fig. 4B). Western blot results were consistent with the IF results (Fig. 4C). In addition, the protein level of TSP-1 increased in human primary urethral scar fibroblasts (Fig. 4C). The expression of circ_0047339 in human primary urethral scar fibroblasts was silenced by transfection of si-circ_0047339 (Fig. 4D). Meanwhile, the expression of miR-4691-5p in si-circ_0047339 group was upregulated than that in si-NC group (Fig. 4D). Western blot results showed that the protein levels of TSP-1, COL-1 and α-SMA were down-regulated in si-circ_0047339 group compared to si-NC group (Fig. 4E). The results of IF were consistent with those of western blot (Fig. 4F). Compared with the si-NC group, the cell viability of si-circ_0047339 group decreased (Fig. 4G). The EDU test results also showed that the cell proliferation in si-circ_0047339 group decreased (Fig. 4H). These results suggested that silencing si-circ_0047339 could reduce the vitality of urethral fibroblasts, inhibit proliferation and alleviate fibrosis.

3.5 Circ_0047339 / miR-4691-5p targeted TSP-1

The targeting relationship between circ_0047339 and miR-4691-5p was analyzed by bioinformatics. Figure 5A showed the targeted binding sites of circ_0047339 and miR-4691-5p. Dual-luciferase assay results showed that miR-4691-5p mimic transfection significantly reduced the activity of circ_0047339-

WT but did not reduce the activity of circ_0047339-MUT (Fig. 5B). TSP-1 was found to contain the potential binding site of miR-4691-5p (Fig. 5C). Then the luciferase reporter plasmid was constructed, which includes 3'UTR regions of TSP-1 mRNA for luciferase detection. The results showed that miR-4691-5p mimic significantly inhibited the translation activity of TSP-1 3'UTR. The TSP-1-3'UTR MUT plasmid was not affected (Fig. 5D). These results suggested that TSP-1 was a target of circ_0047339 / miR-4691-5p. The expression level of TSP-1 mRNA in human primary urethral scar fibroblasts transfected with miR-4691-5p mimic was detected by RT-qPCR. The results showed that TSP-1 mRNA in the miR-4691-5p mimic group was significantly down-regulated compared with mimic-NC group (Fig. 5E). These results further indicated that circ_0047339 could be used as a molecular sponge of miR-4691-5p to regulate the expression of TSP-1.

3.6 Circ_0047339/miR-4691-5p/TSP-1 interaction network was involved in regulating the proliferation, ECM deposition and collagen synthesis of urethral scar fibroblasts

Because circ_0047339 sponged miR-4691-5p, we subsequently determined the role of miR-4691-5p in vitro. miR-4691-5p mimic transfection could inhibit the expression of α-SMA and COL-1 protein in urethral scar fibroblasts, while circ_0047339 overexpression could eliminate this inhibition (Figs. 6A and 6B). These results indicated that circ_0047339/miR-4691-5p interaction regulated ECM deposition and collagen synthesis in urethral scar fibroblasts. As we have proved that TSP-1 is the target of miR-4691-5p, we detected the expression of TSP-1 mRNA and protein by RT-qPCR and western blot. miR-4691-5p mimic transfection could inhibit the expression of TSP-1 in urethral scar fibroblasts, while circ_0047339 overexpression could eliminate this inhibition (Figs. 6B and 6C). In addition, we found that miR-4691-5p mimic transfection could inhibit the vitality and proliferation of urethral scar fibroblasts. Overexpression of circ_0047339 could reverse these results (Figs. 6D and 6E). These results indicated that circ_0047339 / miR-4691-5P / TSP-1 network was involved in the regulation of proliferation, ECM deposition and collagen synthesis of urethral scar fibroblasts.

4 Discussion

In this study, based on the expression profile analysis of circRNA, we identified circ_0047339 as significantly upregulated circRNA in urethral scar tissue. The loss of function experiment showed that circ_0047339 was related to cell viability, proliferation and fibrosis. Circ_0047339 played its role as a ceRNA that competitively bound miR-4691-5p and then eliminated the endogenous inhibition of miR-4691-5p on the target gene TSP-1. The elevated TSP-1 could promote the expression of COL-1 and α-SMA, and then cell proliferation and fibrosis progress. These results revealed that circ_0047339 promoted the growth and fibrosis of urethral scar fibroblasts through the ceRNA mechanism.

At present, there are few research articles on the relationship between circRNA and urethral stricture. The existing literature mainly focuses on renal fibrosis [19, 25]. Other studies have found that circRNA is

related to the mechanism of keloid formation [26–28]. Our study used gene chip technology to analyze the differentially expressed circRNA in urethral scar tissue. We found that compared with the normal control group, there were 130 upregulated circRNA and 166 down-regulated circRNA in urethral scar tissue. In addition, through KEGG pathway analysis, it was found that differentially expressed circRNA was significantly correlated with ECM – receptor interaction. This opens the door for the study of circRNA and urethral stricture, but the relationship between circRNA and the development mechanism of urethral stricture needs further research.

In order to study how differential circRNA participates in the occurrence and development of urethral stricture, we verified its expression in urethral scar tissue. The results showed that the expression of circ_0047339 in human urethral scar tissue was upregulated, and the difference was the most significant. Therefore, we chose circ_0047339 for the follow-up experiment. Urethral scar formation caused by the overactivation of urethral fibroblasts is the core cytobiological event of urethral stricture [29, 30]. We selected urethral fibroblasts to verify the function of circ_0047339. The results showed that circ_0047339 was significantly overexpressed in urethral scar fibroblasts compared with normal urethral fibroblasts. By silencing the expression of circ_0047339, we found that the cell viability, proliferation, and expression of α-SMA and COL-1 of urethral scar fibroblasts decreased. This was consistent with previous results [31]. This evidence suggested that circ_0047339 might participate in urethral stricture by influencing the growth of urethral scar fibroblasts, ECM deposition, and collagen synthesis. It was recommended that circ_0047339 might play an important role in the occurrence and development of urethral stricture.

The research on the biological function mechanism of circRNA has made rapid progress. Among them, circRNA pays the most attention to the function of the miRNA sponge [32, 33]. For example, circPTPN12 promotes keloid fibroblasts' growth by activating the Wnt pathway targeted by sponge miR-21-5p [34]. Through luciferase reporter gene detection, we found that circ_0047339 could inhibit the expression of miR-4691-5p through the sponge. MiR-4691-5p can promote the development of liver cancer [35], but it has not been studied in urethral stricture. Our study found that miR-4691-5p was down-regulated in urethral scar tissue and fibroblasts compared with the control group. TSP-1 is a regulatory factor that promotes the process of fibrosis, and TGF-β1 can be activated by TSP-1, thus promoting ECM deposition and collagen synthesis [36, 37]. Inhibition of TSP-1 expression has been proved to inhibit hypertrophic scar development [38, 39]. Here, using luciferase reporter gene detection, we found that the translation activity of TSP-1 3'UTR was significantly inhibited by miR-4691-5p mimic, which indicated that TSP-1 was a target of miR-4691-5p. Transfection of miR-4691-5p mimic could inhibit the expression of TSP-1 in urethral scar fibroblasts. At the same time, over-expression of circ_0047339 could reverse its inhibition, suggesting that circ_0047339 could be used as a molecular sponge of miR-4691-5p to regulate the expression of TSP-1. In addition, mimic transfection of miR-4691-5p could inhibit the vitality and proliferation of urethral scar fibroblasts. It could inhibit the expression of α-SMA and COL-1, but the inhibition disappears after overexpression of mir-4691-5p. These results suggested that circ_0047339/miR-4691-5p/TSP-1 network participates in the growth and activation of urethral scar fibroblasts.

It is important to emphasize some limitations related to this study. In this study, only circ_0047339 was verified. The expression profile of other circRNAs in urethral stricture remains to be explored.

5 Conclusion

Our research showed that circRNA could regulate the development of urethral stricture. Circ_0047339 was upregulated in human urethral scar tissue and urethral scar fibroblasts. Circ_0047339 silence could inhibit the proliferation of urethral scar fibroblasts and the expression of α-SMA and COL-1. Circ_0047339 regulated fibroblast proliferation, ECM deposition and collagen synthesis by increasing TSP-1 expression as an endogenous miR-4691-5p sponge.

Declarations

Conflict of Interest

There is no conflict of interest.

Acknowledgments

This work was supported by all of the authors.

Ethics Approval Statement

The procedure used in this research was approved by Medical Ethics Committee of Xiangya Hospital Central South University.

References

1. Hillary, C.J., N.I. Osman, and C.R. Chapple, *Current trends in urethral stricture management*. Asian J Urol, 2014. **1**(1): p. 46–54.
2. Tritschler, S., et al., *Urethral stricture: etiology, investigation and treatments*. Dtsch Arztebl Int, 2013. **110**(13): p. 220–6.
3. Alwaal, A., et al., *Epidemiology of urethral strictures*. Transl Androl Urol, 2014. **3**(2): p. 209–13.
4. Frankel, J.K. and G.P. Murphy, *International volunteerism and urethral stricture disease: a review*. Transl Androl Urol, 2018. **7**(4): p. 659–665.
5. Chapple, C., et al., *SIU/ICUD Consultation on Urethral Strictures: The management of anterior urethral stricture disease using substitution urethroplasty*. Urology, 2014. **83**(3 Suppl): p. S31-47.
6. Strittmatter, F., et al., *[Urethral stricture: From diagnostics to appropriate treatment]*. Urologe A, 2017. **56**(8): p. 1047–1057.
7. Buckley, J.C., et al., *SIU/ICUD Consultation on Urethral Strictures: Dilation, internal urethrotomy, and stenting of male anterior urethral strictures*. Urology, 2014. **83**(3 Suppl): p. S18-22.

8. Santucci, R. and L. Eisenberg, *Urethrotomy has a much lower success rate than previously reported*. J Urol, 2010. **183**(5): p. 1859–62.
9. Ofoha, C.G., et al., *Predictors of urethral stricture recurrence following urethroplasty: a retrospective review at the Jos University Teaching Hospital, Nigeria.* Pan Afr Med J, 2019. **32**: p. 190.
10. Cotter, K.J., et al., *Trends in Urethral Stricture Disease Etiology and Urethroplasty Technique From a Multi-institutional Surgical Outcomes Research Group*. Urology, 2019. **130**: p. 167–174.
11. Hong, M.K.H., et al., *Male urethral stricture disease in a regional centre: 10 years of experience*. ANZ J Surg, 2019. **89**(6): p. 747–751.
12. Cavalcanti, A.G., et al., *A morphometric analysis of bulbar urethral strictures*. BJU Int, 2007. **100**(2): p. 397–402.
13. Adams, J.C. and J. Lawler, *The thrombospondins*. Cold Spring Harb Perspect Biol, 2011. **3**(10): p. a009712.
14. Bige, N., et al., *Thrombospondin-1 plays a profibrotic and pro-inflammatory role during ureteric obstruction*. Kidney Int, 2012. **81**(12): p. 1226–38.
15. Murphy-Ullrich, J.E. and M.J. Suto, *Thrombospondin-1 regulation of latent TGF-β activation: A therapeutic target for fibrotic disease*. Matrix Biol, 2018. **68–69**: p. 28–43.
16. Sun, D., et al., *Thrombospondin-1 short hairpin RNA suppresses tubulointerstitial fibrosis in the kidney of ureteral obstruction by ameliorating peritubular capillary injury*. Kidney Blood Press Res, 2012. **35**(1): p. 35–47.
17. Jiang, X. and Q. Ning, *Circular RNAs as novel regulators, biomarkers and potential therapies in fibrosis*. Epigenomics, 2019. **11**(9): p. 1107–1116.
18. Dai, X., et al., *Role of circular RNAs in visceral organ fibrosis*. Food Chem Toxicol, 2021. **150**: p. 112074.
19. Huang, J., et al., *Identification of circular RNA expression profiles in renal fibrosis induced by obstructive injury*. Ren Fail, 2021. **43**(1): p. 1368–1377.
20. Zhou, Y., et al., *Differential expression of circular RNAs in hepatic tissue in a model of liver fibrosis and functional analysis of their target genes*. Hepatol Res, 2019. **49**(3): p. 324–334.
21. Zhou, B. and J.W. Yu, *A novel identified circular RNA, circRNA_010567, promotes myocardial fibrosis via suppressing miR-141 by targeting TGF-β1*. Biochem Biophys Res Commun, 2017. **487**(4): p. 769–775.
22. Hu, W., et al., *Circular RNA circRNA_15698 aggravates the extracellular matrix of diabetic nephropathy mesangial cells via miR-185/TGF-β1*. J Cell Physiol, 2019. **234**(2): p. 1469–1476.
23. Zhang, L., et al., *Lung myofibroblast transition and fibrosis is regulated by circ0044226*. Int J Biochem Cell Biol, 2020. **118**: p. 105660.
24. Wang, Q., et al., *Hsa_circ_0092276 promotes doxorubicin resistance in breast cancer cells by regulating autophagy via miR-348/ATG7 axis*. Transl Oncol, 2021. **14**(8): p. 101045.

25. Wei, L., et al., *Integrated Analysis of the CircRNA-Based ceRNA Network in Renal Fibrosis Induced by Ischemia Reperfusion Injury*. Front Genet, 2021. **12**: p. 793182.
26. Ge, X., et al., *Circular RNA HECTD1 knockdown inhibits transforming growth factor-beta/ small mothers against decapentaplegic (TGF-β/Smad) signaling to reduce hypertrophic scar fibrosis*. Bioengineered, 2022. **13**(3): p. 7303–7315.
27. Li, X., et al., *Identification of crucial noncoding RNAs and mRNAs in hypertrophic scars via RNA sequencing*. FEBS Open Bio, 2021. **11**(6): p. 1673–1684.
28. Wang, B., et al., *circNRIP1 facilitates keloid progression via FXR1–mediated upregulation of miR–503–3p and miR–503–5p*. Int J Mol Med, 2021. **47**(5).
29. Huang, S., et al., *Effect of dual mTOR inhibitor on TGFβ1-induced fibrosis in primary human urethral scar fibroblasts*. Biomed Pharmacother, 2018. **106**: p. 1182–1187.
30. Xu, N., et al., *Fasudil inhibits proliferation and collagen synthesis and induces apoptosis of human fibroblasts derived from urethral scar via the Rho/ROCK signaling pathway*. Am J Transl Res, 2017. **9**(3): p. 1317–1325.
31. Sa, Y., et al., *TIMP-1 Induces α-Smooth Muscle Actin in Fibroblasts to Promote Urethral Scar Formation*. Cell Physiol Biochem, 2015. **35**(6): p. 2233–43.
32. Wilusz, J.E. and P.A. Sharp, *Molecular biology. A circuitous route to noncoding RNA*. Science, 2013. **340**(6131): p. 440–1.
33. Thomas, L.F. and P. Sætrom, *Circular RNAs are depleted of polymorphisms at microRNA binding sites*. Bioinformatics, 2014. **30**(16): p. 2243–6.
34. Liu, F., T. Li, and X. Zhan, *Silencing circular RNAPTPN12 promoted the growth of keloid fibroblasts by activating Wnt signaling pathway via targeting microRNA-21-5p.* Bioengineered, 2022. **13**(2): p. 3503–3515.
35. Choi, J.H., et al., *TPRG1-AS1 induces RBM24 expression and inhibits liver cancer progression by sponging miR-4691-5p and miR-3659*. Liver Int, 2021. **41**(11): p. 2788–2800.
36. Xiao, J., et al., *hsa-miR-4443 inhibits myocardial fibroblast proliferation by targeting THBS1 to regulate TGF-β1/α-SMA/collagen signaling in atrial fibrillation*. Braz J Med Biol Res, 2021. **54**(4): p. e10692.
37. Zhou, Y., et al., *microRNA-221 Inhibits Latent TGF-β1 Activation through Targeting Thrombospondin-1 to Attenuate Kidney Failure-Induced Cardiac Fibrosis*. Mol Ther Nucleic Acids, 2020. **22**: p. 803–814.
38. Jiang, D., et al., *miR-205 inhibits the development of hypertrophic scars by targeting THBS1*. Aging (Albany NY), 2020. **12**(21): p. 22046–22058.
39. Xu, X., et al., *Investigating the potential of LSKL peptide as a novel hypertrophic scar treatment*. Biomed Pharmacother, 2020. **124**: p. 109824.

Figures

Figure 1

CircRNA expression profile analysis of urethral scar tissue. A. Principal Component Analysis 3D diagram showed three principal components in three-dimensional space, PC1 was the first principal component, PC2 was the second principal component, and PC3 was the third principal component. The percentage in the coordinate axis was the contribution rate of each principal component. Duplicate samples of the same group were marked with the same shape and color. B. Scatter chart showed the signal values of circRNA in each group of samples. C. Volcano map showed the difference of circRNA in two groups of samples. Up-regulated circRNA was marked in red, down-regulated circRNA was marked in green, and circRNA with no significant difference was marked in black.

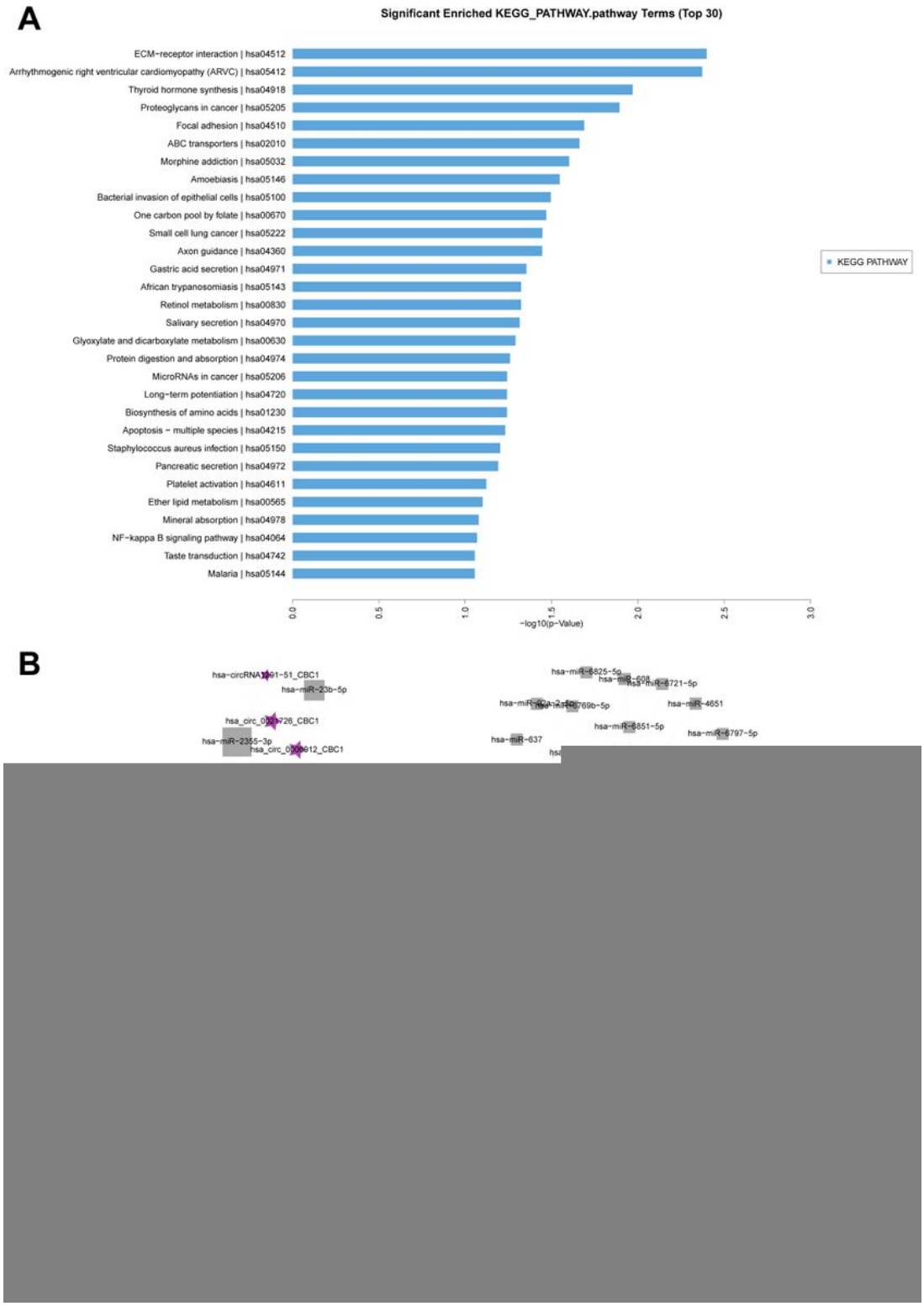

Figure 2

Interaction between circRNA and miRNA in urethral scar tissue. A. KEGG showed the enrichment of differential circRNA functional pathways. B. circRNA-miRNA interaction analysis network diagram. Square represented miRNA, and pentagram represented circRNA, in which green was down-regulated and purple was upregulated. The size of a point meant the number of nodes connected to the point, and the larger the point, the more nodes connected to the point.

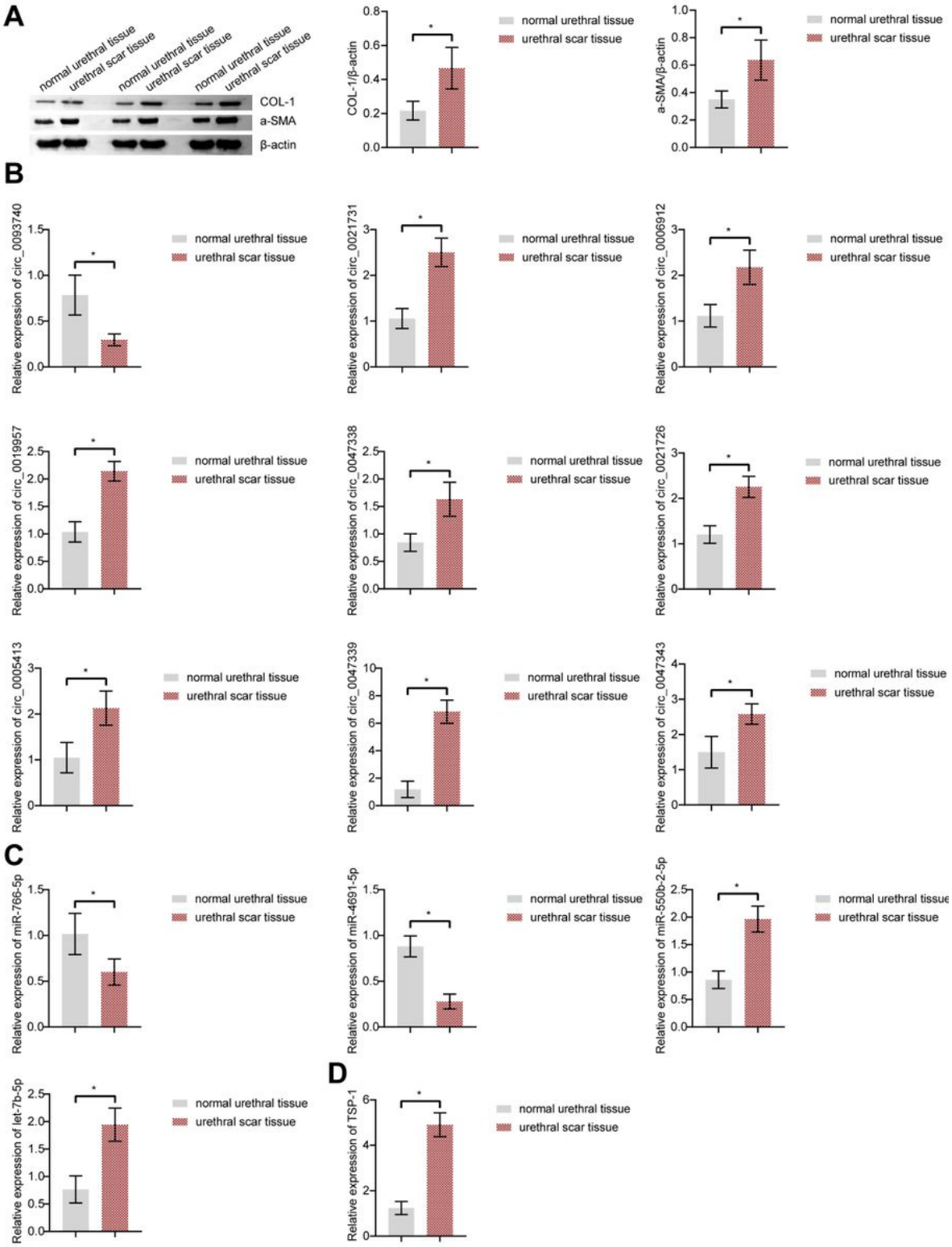

Figure 3

The expression of circ_0047339 /miRNA/TSP-1 interaction in urethral scar tissue. A. We performed western blot to verify the expression of COL-1 and α-SMA in urethral scar tissue. B. We confirmed the expression of the first nine differential circRNA in the chip microarray analysis by RT-qPCR. C. The expression of let-7b-5p, miR-4691-5p, miR-766-5p and miR-550b-2-5p were characterized by RT-qPCR in urethral scar tissue. D. The expression of TSP-1 in urethral scar tissue was verified by RT-qPCR. *P<0.05.

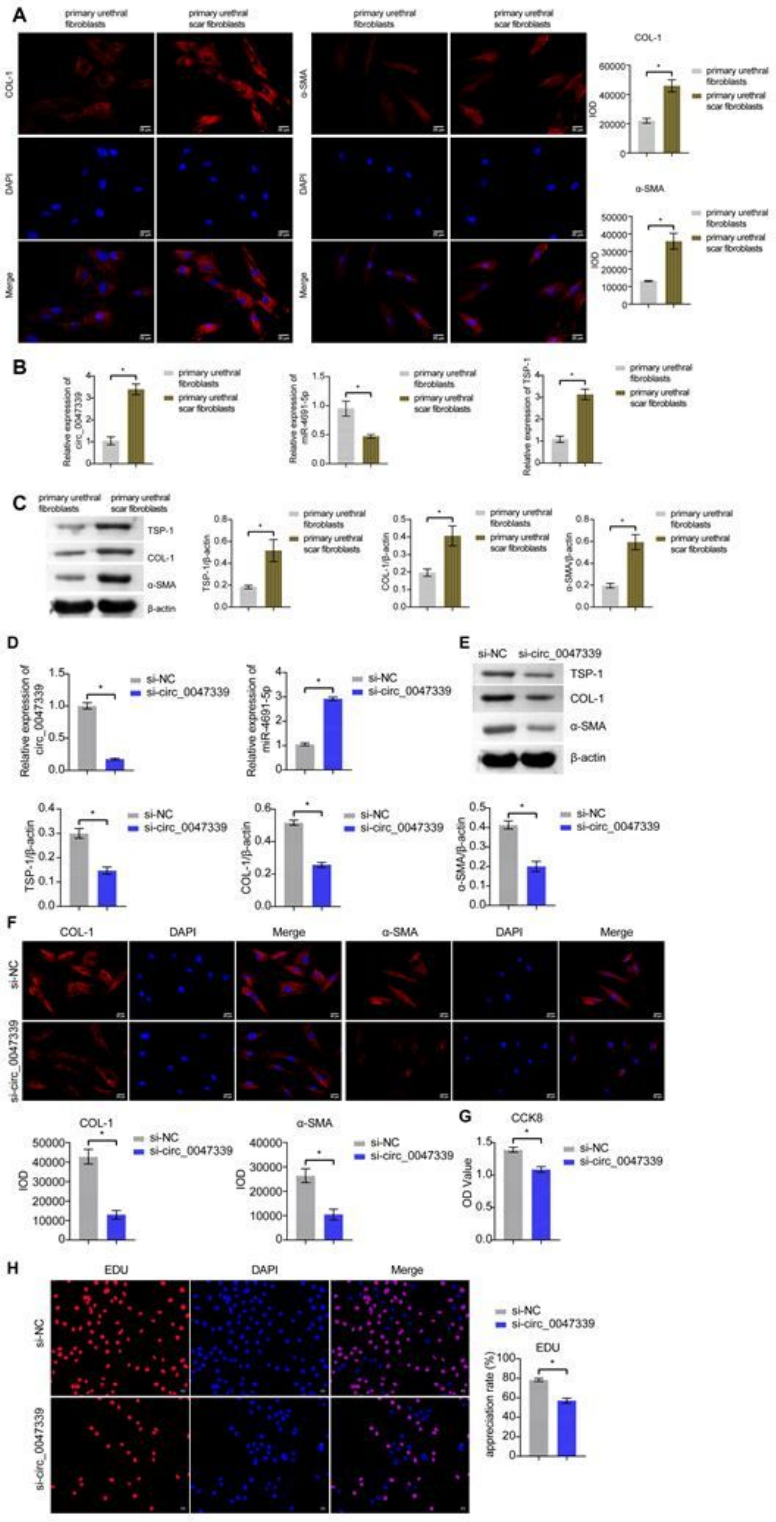

Figure 4

Circ_0047339 regulated the fibrosis of urethral fibroblasts. A. The expressions of COL-1 and α-SMA were detected by IF. B. RT-qPCR was used to detect the expression of circ_0047339, miR-4691-5p and TSP-1. C. Western blot was conducted to determine the protein expression of TSP-1, COL-1, and α-SMA. D. The expression of circ_0047339 and miR-4691-5p was investigated by RT-qPCR. E. Western blot was conducted to determine the protein expression of COL-1, α-SMA and TSP-1. F. The expression of COL-1

and α-SMA was assessed by IF. G. CCK-8 was used to detect the cell viability. H. EDU assay was utilized to detect cell proliferation. *P<0.05.

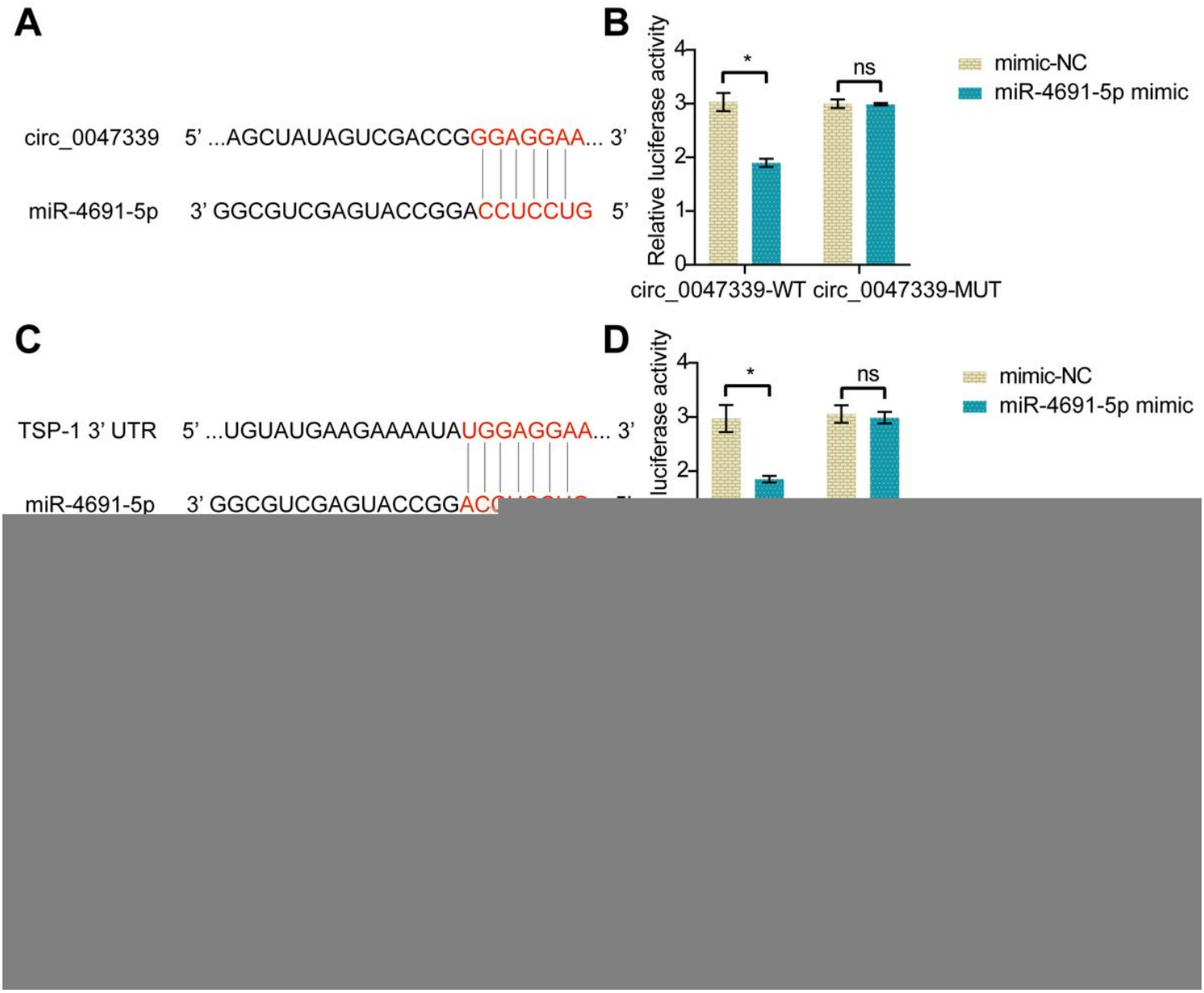

Figure 5

Circ_0047339 /miR-4691-5p targeted TSP-1. A. The binding site of circ_0047339 and miR-4691-5p. B. Dual-luciferase assay was confirmed that circ_0047339 was target miR-4691-5p. C. The binding site of miR-4691-5p and TSP-1. D. Dual-luciferase assay was assessed that TSP-1 targets miR-4691-5p. E. RT-qPCR was used to detect the expression of miR-4691-5p and TSP-1. *P<0.05. ns means no significance.

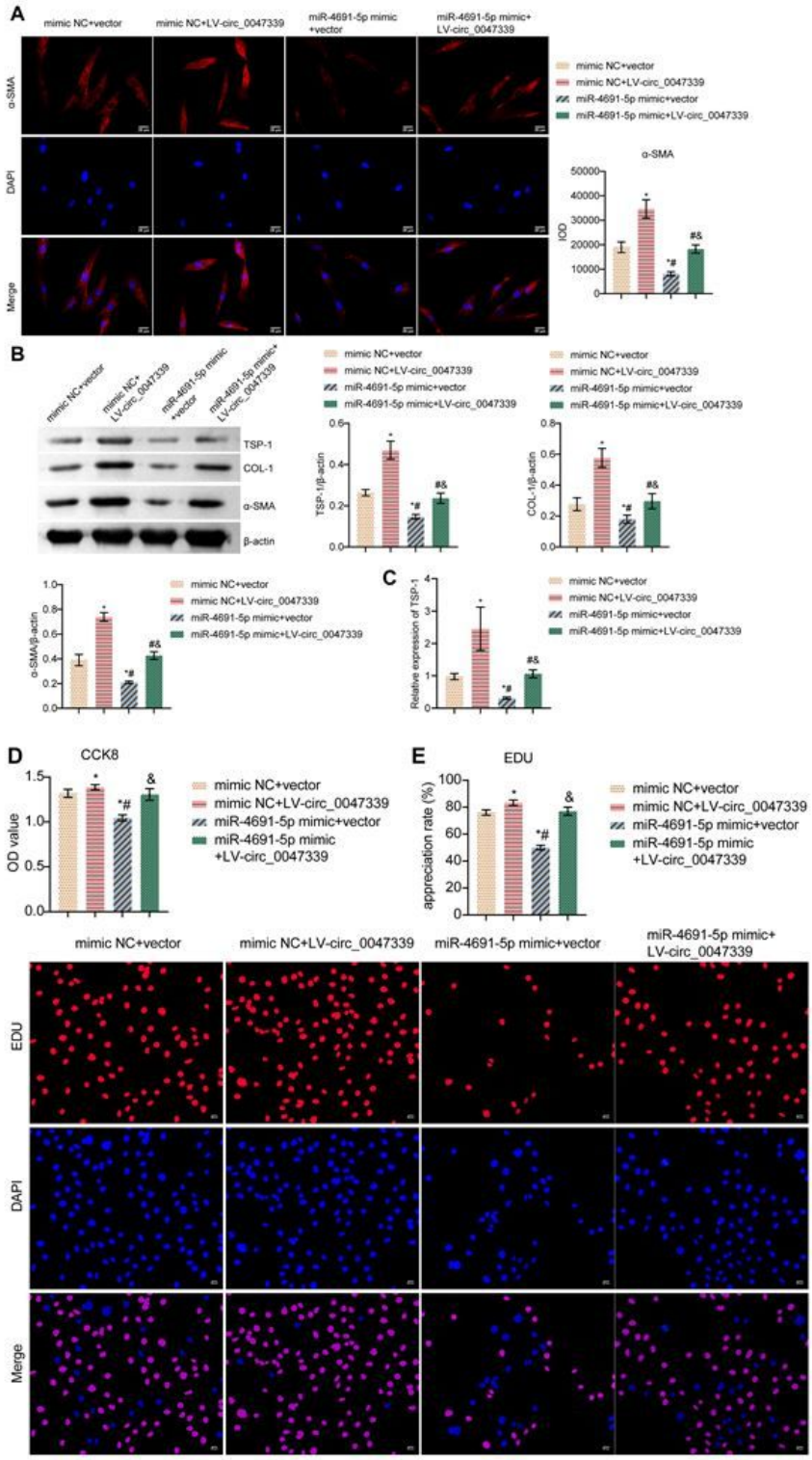

Figure 6

Circ_0047339/miR-4691-5p/TSP-1 interaction network regulated the proliferation, ECM deposition and collagen synthesis of urethral scar fibroblasts. A. The expressions of α-SMA were evaluated by IF. B. The protein expression of COL-1, α-SMA and TSP-1 was tested by western blot. C. RT-qPCR was used to assess the expression of TSP-1. D. The cell viability was investigated by CCK-8. E. EDU assay was used to

investigate cell proliferation. *P<0.05, VS mimic NC+ vector group. #P<0.05, VS mimic NC+ LV-circ_0047339 group. &P<0.05, VS miR-4691-5p mimic+ vector group.